Available online at www.sciencedirect.com
ScienceDirect
Ceramics International 38S (2012) S525–S528
CERAMICS INTERNATIONAL
www.elsevier.com/locate/ceramint

A study on the incorporation of ZnO nanoparticles into MEH-PPV based organic–inorganic hybrid solar cells

Yong-June Choi [a], Hyung-Ho Park [a,*], Stephen Golledge [b], David C. Johnson [c]

[a] Department of Materials Science and Engineering, Yonsei University, Seoul 120-749, Republic of Korea
[b] CAMCOR, University of Oregon, Eugene, OR 97403-1241, USA
[c] Department of Chemistry and the Materials Science Institute, University of Oregon, Eugene, OR 97403, USA

Available online 24 May 2011

Abstract

A conjugated polymer MEH-PPV [poly(2-methoxy-5-(2′-ethylhexyloxy)-p-phenylene vinylene)] and ZnO inorganic semiconductor nanoparticles were blended to form bulk heterojunction organic–inorganic hybrid solar cells. The simple photovoltaic device could be fabricated by spin-coating and the architecture was glass/ITO/MEH-PPV/Al or glass/ITO/MEH-PPV:ZnO nanoparticles (0, 5, 20, and 30 wt% to MEH-PPV)/Al. We could obtain the short-circuit current density (J_{SC}), open-circuit voltage (V_{OC}), and fill factor (FF) were, respectively, 0.0081 mA/cm^2, 0.606 V, and 17.6% for pristine MEH-PPV as used a single active layer and also 0.0120 mA/cm^2, 0.858 V, and 20.2% for MEH-PPV:30 wt% ZnO nanocomposite as used a hybrid active layer. This enhancement of J_{SC}, V_{OC}, and FF was explained by the preservation of optical quality for hybrid active layer and facile electron injection from the introduction of ZnO semiconductor nanoparticles.

Keywords: B. Surfaces; C. Optical properties; D. ZnO; E. Functional applications

1. Introduction

Organic photovoltaic cells have been researched very intensively because they have a lot of advantages comparing with inorganic Si-based solar cells. Among all alternative technologies to Si-based pn-junction solar cells, organic solar cells could lead the most significant cost reduction and realize flexible devices [1]. Bulk heterojunction (BHJ) structure has been introduced by many research groups in recent years [2]. For example, the BHJ photovoltaic devices have been reported using the polymer composites [3] or conjugated polymers with fullerenes [4]. However, the BHJ structure using polymer composites or conjugated polymers with fullerenes has the limits, which are the recombination interaction between organic electron donor and acceptor, uncontrolled interfacial structure between active layer and electrode, and also unbalanced charge-carrier mobilities among electrons and holes. To overcome these limitations, we investigated the organic–inorganic hybrid BHJ photovoltaic cells using ZnO nanoparticles as an inorganic acceptor and MEH-PPV as an organic donor. These hybrid cells give a solution to overcome charge-transport limitation via conjugated polymer by utilizing the high electron mobility of the inorganic phase [5]. Furthermore, it is possible to improve the charge transfer and the facile electron injection in the interface between donor and acceptor through the distribution of 50 nm-nanoparticles in the exciton diffusion length of MEH-PPV [6].

In this study, the effects of the amounts of incorporated ZnO nanoparticles on the formation of the blended active layer and changes of photovoltaic properties by the introduction of ZnO nanoparticles into MEH-PPV were investigated. The observation would be reached to the discussion on the related photovoltaic properties of the modified active layer.

2. Experimental

Materials used as active layer were MEH-PPV and ZnO nanoparticles. MEH-PPV, which was purchased from Sigma–Aldrich, Inc., has the number average molecular weight, Mn = (1.5–2.5) × 10^5 and a polydispersity (Mw/Mn) of about 5. ZnO nanoparticles were purchased from Sigma–Aldrich, Inc.

* Corresponding author. Tel.: +82 2 21232853; fax: +82 2 3125375.
E-mail address: hhpark@yonsei.ac.kr (H.-H. Park).

0272-8842/$36.00
doi:10.1016/j.ceramint.2011.05.068

and the average diameter of particles was about 50 nm. For device preparation, glass substrates with an indium-tin oxide (ITO) electrode (~150 nm thickness, $11.5 \pm 3\ \Omega/\square$) were cleaned by routine procedure. The composite layer of solar cells was prepared from blend solution of MEH-PPV (6 mg/mL):ZnO nanoparticles (0, 5, 20, and 30 wt% to MEH-PPV) into toluene solution. The blending solutions for active layer were spin-coated onto ITO coated glass substrates at a spinning speed of 2000 rpm for 30 s and heated at 100 °C on hot plate in N_2 atmosphere glove box for 1 h. The thickness of active layer was around 100 nm for all the samples measured by atomic force microscopy (AFM: VEECO D03100). 120 nm thick aluminum (Al) electrode was thermally deposited. Fig. 1 shows the schematic device architecture (a) and the energy level diagram (b). In the final device, the dimension of active layer was 2 mm × 2 mm. The depth profiling was reported using X-ray photoelectron spectroscopy (XPS: Thermo Scientific ESCALAB 250) with ion beam energy of 3 kV and 2 μA. We measured the transmission electron microscopy (TEM: JEOL JEM-2100F) by drying the solution of ZnO nanoparticles or MEH-PPV:ZnO blend on a carbon-coated copper grid. Optical absorbance was monitored using an ultraviolet–visible–near infrared (UV–vis–NIR) spectrophotometer (JASCO UV-570), and the topography for surface of the active layer was analyzed using atomic force microscopy (AFM: VEECO D03100). Current density–voltage (J–V) experiments were performed on MEH-PPV and MEH-PPV:ZnO nanoparticles composite films using HP4145B. The short circuit current density (J_{SC}) and open circuit voltage (V_{OC}) characteristics of the devices were accomplished using a Keithley 2400 source meter. The photovoltaic performance of devices was calculated from the J_{SC}–V_{OC} characteristics under air mass (AM) 1.5 solar simulated light irradiation of 100 mW/cm^2.

3. Results and discussion

We introduced ZnO nanoparticles as the n-type inorganic semiconductor and MEH-PPV as the p-type organic semiconducting polymer in organic–inorganic hybrid solar cells. Fig. 1(c) and (d) shows TEM images of ZnO nanoparticles and 5 wt% of ZnO nanoparticles in MEH-PPV matrix, respectively. We could observe average particle size was about 40–60 nm and well-distribution of ZnO nanoparticles into MEH-PPV matrix.

In order to confirm the uniform distribution of ZnO nanoparticles in MEH-PPV matrix, after each sputtering cycle (60 s, 16 cycles), the XPS depth profiling analysis has also been done. Fig. 2 shows an evolution in time of the XPS Zn 2p peaks during subsequent etch time by relative intensity and the atomic concentration plot of C, O, In, Sn, and Zn as a function of etch times. It is visible that, with increasing sputtering time, Zn 2p peaks are almost same intensity among total sputtering time except the primary surface (no etch, 0 s) as shown in Fig. 2(a). This result clarifies the fact that ZnO nanoparticles are distributed well in MEH-PPV:ZnO nanoparticles composite layer (Fig. 2(b)).

Fig. 3 shows changes of the optical density according to various contents of ZnO nanoparticles and the absorbance of ZnO nanoparticles. The pristine MEH-PPV exhibits a broad absorption spectrum peaking at about 502 nm and a small absorption peak around 330 nm. With ZnO nanoparticles, the optical density of MEH-PPV:ZnO nanocomposite films was

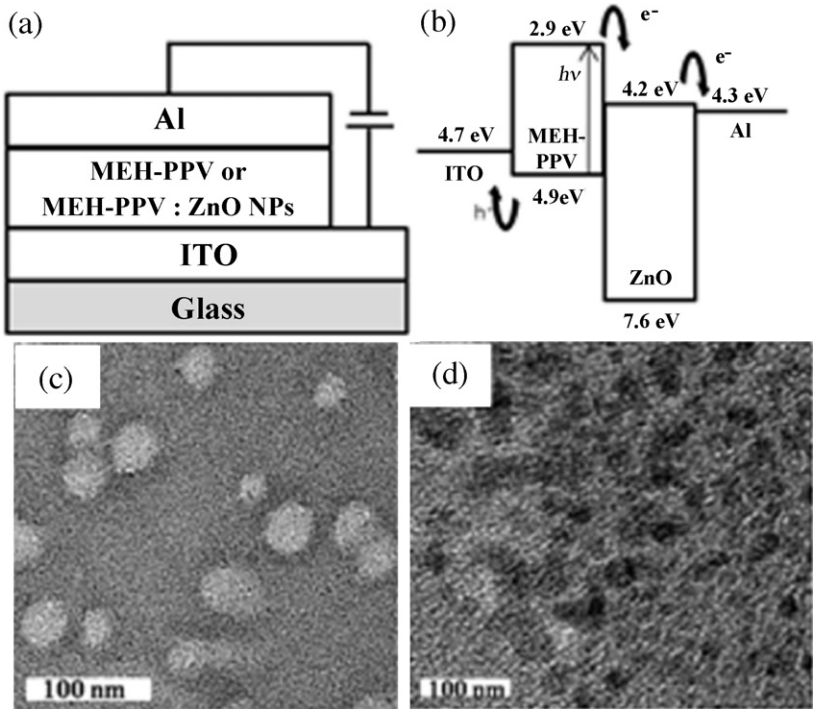

Fig. 1. (a) The schematic device architecture and (b) energy level diagram. (c) The TEM images of ZnO nanoparticles and (d) MEH-PPV with 5 wt% ZnO nanoparticles.

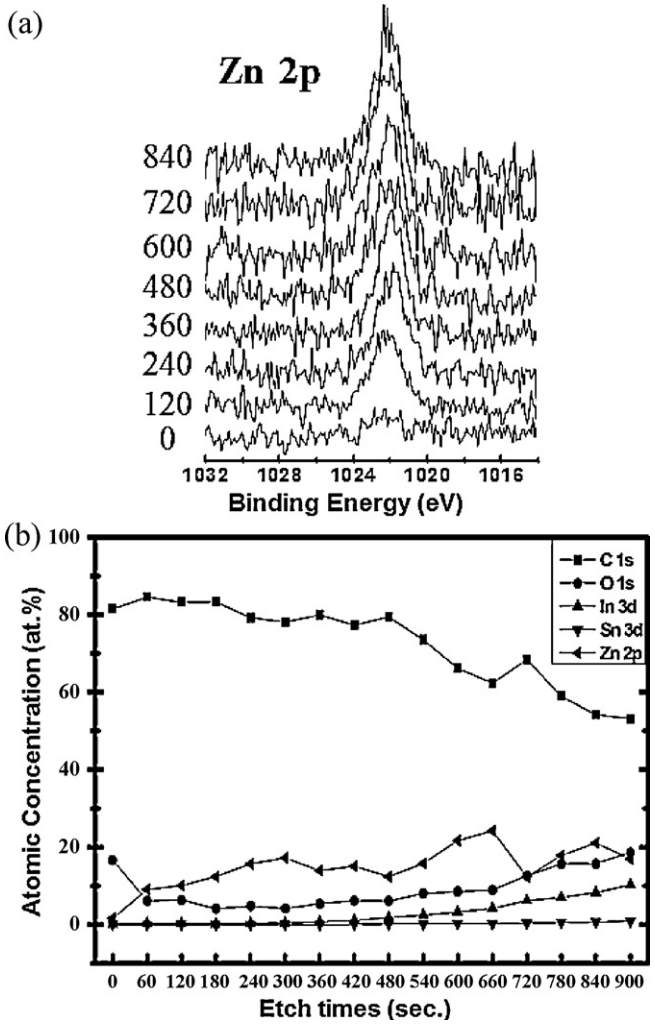

Fig. 2. (a) An evolution in time of Zn 2p photoelectron spectra during subsequent etch time by relative intensity; (b) the atomic concentration of C 1s, O 1s, In 3d, Sn 3d, and Zn 2p as a function of etch times.

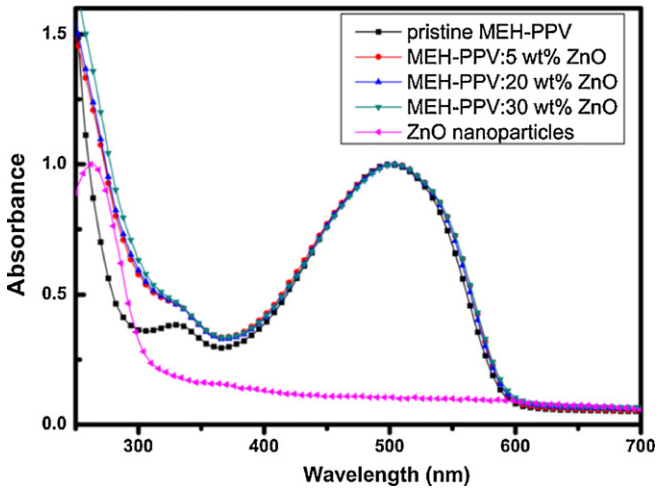

Fig. 3. UV–vis absorption of ZnO nanoparticles and the various blends of MEH-PPV with 0, 5, 20, and 30 wt% ZnO nanoparticles.

slightly increased below 400 nm by combining with the absorption of ZnO nanoparticles. But the maximum density at 502 nm was not changed because the thickness of the films could be controlled same as around 100 nm [7]. This result provides the incorporation of ZnO nanoparticles into MEH-PPV does not lead to degrade the optical quality of the composite films [8].

To investigate of spatial effect by the incorporation of ZnO nanoparticles into MEH-PPV on the device performance, the topographies of MEH-PPV and MEH-PPV with 5, 20, and 30 wt% ZnO nanoparticles were observed using non-contact mode AFM. The roughness value of the MEH-PPV film surface was 0.461 nm. Meanwhile, the roughness values of the MEH-PPV: 5, 20, and 30 wt% ZnO nanoparticles were 0.569, 0.605, and 0.632 nm, respectively. Fig. 4 corresponds to 500 nm × 500 nm AFM image. The surface of the nanocomposite film was slightly rougher than that of MEH-PPV film due to the presence of relative large size ZnO nanoparticles. This roughened surface induces a variation in the thickness of the device and an enhanced applied field may be developed at the thinner regions of the films. A rougher interface between active layer and cathode may give rise to an increase in the effective surface area with a resulting electron injection for the device [9]. Furthermore, an introduction of ZnO nanoparticles induced a close packing of MEH-PPV to increase an overlap of π orbital and result in an enhancement of polymer conductivity [10]. This steric effect of ZnO nanoparticles could be identified

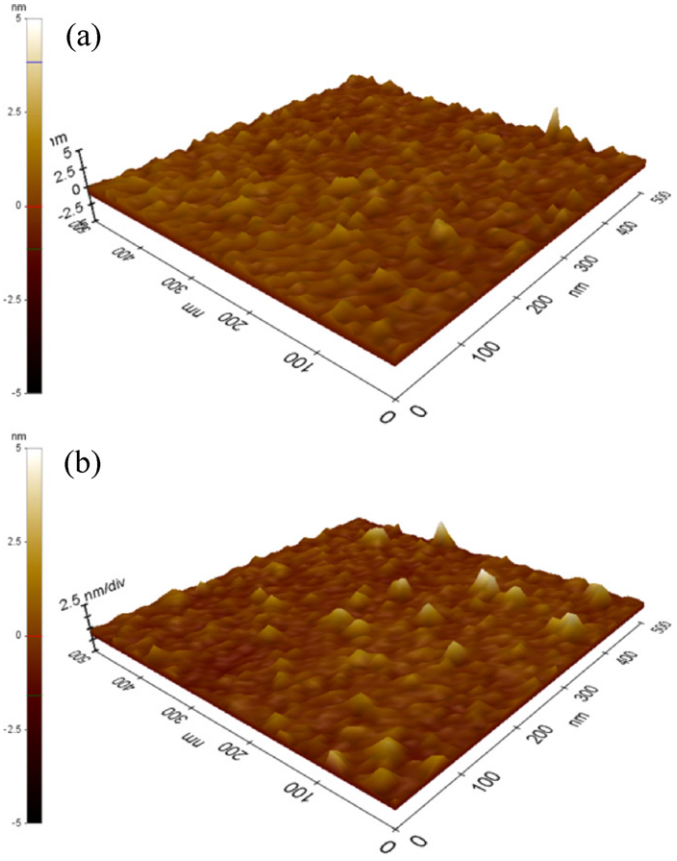

Fig. 4. AFM images of (a) MEH-PPV and (b) MEH-PPV composite film with 30 wt% ZnO nanoparticles.

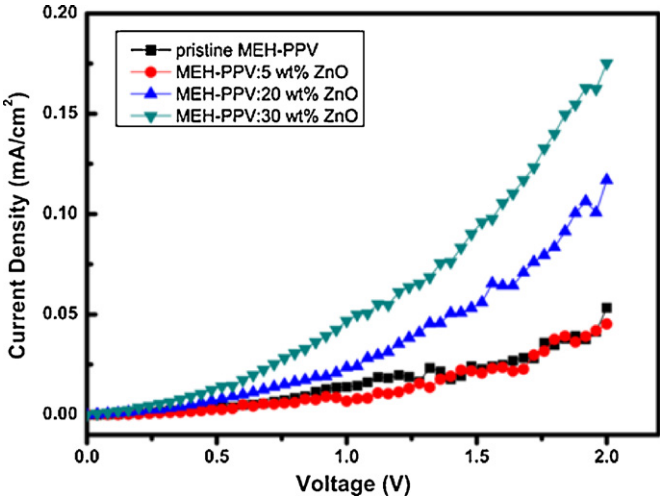

Fig. 5. Current density–voltage curves for the MEH-PPV and MEH-PPV:ZnO nanocomposite films.

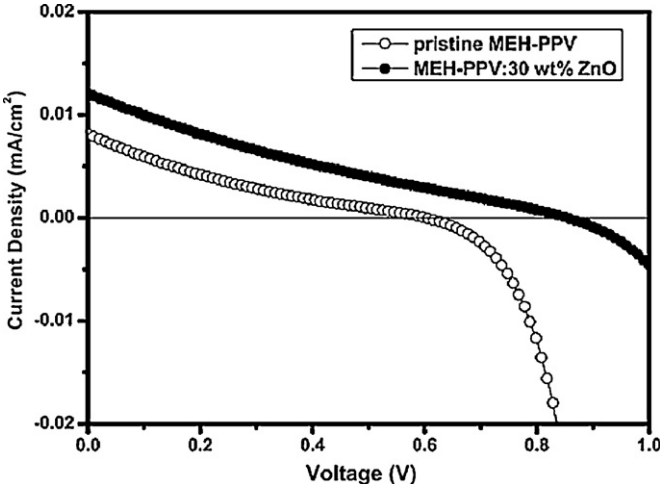

Fig. 6. Plot of current density–voltage curves for the MEH-PPV and MEH-PPV film with 30 wt% ZnO nanoparticles under 100 mW/cm^2 illumination (AM 1.5).

by the enhancement of *J–V* characteristics of device in dark condition. Fig. 5 shows the current density and voltage characteristics of MEH-PPV and MEH-PPV:ZnO nanocomposite films. Enhanced current density in MEH-PPV composite films with 20 and 30 wt% ZnO nanoparticles was obtained by incorporation of enough amounts of ZnO nanoparticles. This result is affected by an effective electron transfer via n-type semiconducting ZnO nanoparticles to cathode as an intrinsic effect and the increase of effective area between active layer and electrode to inject electrons from rising surface roughness of the films [9].

We could obtain the photovoltaic performances of MEH-PPV and MEH-PPV with 30 wt% ZnO nanoparticles as shown in Fig. 6. The values of J_{SC}, V_{OC}, and FF were 0.0081 mA/cm^2, 0.606 V, and 17.6% for pristine MEH-PPV single layer device and also 0.0120 mA/cm^2, 0.858 V, and 20.2% for MEH-PPV with 30 wt% ZnO nanoparticles, respectively. The power conversion efficiency of devices are remained low values in this work, which is used MEH-PPV as an active layer of organic solar cells, however, the device performance such as J_{SC}, V_{OC}, and FF can be slightly enhanced with the incorporation of ZnO nanoparticles into MEH-PPV.

4. Conclusions

In this study, ZnO nanoparticles and MEH-PPV composite layer has been fabricated as an active layer for solar cells. And also, well-distributed ZnO nanoparticles in composite layer are clarified by the XPS depth profiling analysis and TEM images. We can suggest the roles of ZnO nanoparticles into MEH-PPV as an active layer of organic–inorganic hybrid solar cells by the conservation of optical quality for hybrid active layer and steric effect to the films. Finally, the device performance could be enhanced by the incorporation of ZnO nanoparticles in MEH-PPV for application of organic–inorganic hybrid solar cells.

Acknowledgements

This research was supported by Future-based Technology Development Program (Nano Fields) through the National Research Foundation of Korea (NRF) funded by the Ministry of Education, Science and Technology (2009-0082604). Experiments at PLS were supported in part by MEST and POSTECH.

References

[1] J.-M. Nunzi, Organic photovoltaic materials and devices, Comptes Rendus Physique 3 (2002) 523–542.
[2] P. Madakasira, K. Inoue, R. Ulbricht, S.B. Lee, M. Zhou, J.P. Ferraris, A.A. Zakhidov, Multilayer encapsulation of plastic photovoltaic devices, Synthetic Metals 155 (2005) 332–335.
[3] J.J.M. Halls, C.A. Walsh, N.C. Greenham, E.A. Marseglia, R.H. Friend, S.C. Moratti, A.B. Holmes, Efficient photodiodes from interpenetrating polymer networks, Nature 376 (1995) 498–500.
[4] G. Yu, J. Gao, J.C. Hummelen, F. Wudl, A.J. Heeger, Polymer photovoltaic cells: enhanced efficiencies via a network of internal donor–acceptor heterojunctions, Science 270 (1995) 1789–1791.
[5] W.J.E. Beek, M.M. Wienk, R.A.J. Janssen, Efficient hybrid solar cells from zinc oxide nanoparticles and a conjugated polymer, Advanced Materials 16 (2004) 1009–1013.
[6] T.J. Savenije, J.M. Warman, A. Goossens, Visible light sensitisation of titanium dioxide using a phenylene vinylene polymer, Chemical Physics Letters 287 (1998) 148–153.
[7] W.J.E. Beek, M.M. Wienk, M. Kemerink, X. Yang, R.A.J. Janssen, Hybrid zinc oxide conjugated polymer bulk heterojunction solar cells, Journal of Physical Chemistry B 109 (2005) 9505–9516.
[8] T.-F. Guo, G.L. Pakhomov, T.-C. Wen, X.-G. Chin, S.-H. Liou, Effect of TiO_2 nanoparticles on polymer-based bulk heterojunction solar cells, Japanese Journal of Applied Physics 45 (2006) L1314–L1316.
[9] S.A. Carter, J.C. Scott, P.J. Brock, Enhanced luminance in polymer composite light emitting devices, Applied Physics Letters 71 (1997) 1145–1147.
[10] S.-J. Wang, H.-H. Park, Electronic properties of hybridized poly (3,4-ethylenedioxythiophene): polystyrene sulfonate with surface-capped CdSe nanocrystals, Journal of Applied Physics 105 (2009) 023716.